

Multiple-step martensitic transformations in the $\text{Ni}_{51}\text{Ti}_{49}$ single crystal

Jafar Khalil-Allafi · Behnam Amin-Ahmadi

Received: 3 April 2010 / Accepted: 18 June 2010 / Published online: 1 July 2010
© Springer Science+Business Media, LLC 2010

Abstract Multiple-step martensitic transformations of an aged $\text{Ni}_{51}\text{Ti}_{49}$ single crystal using calorimetric method were investigated. Results show that for short aging times (10–45 min) multiple-step martensitic transformations on cooling occur in two steps. Applying intermediate aging times (1.25–4 h) results in three steps and long aging times (more than 8 h) lead to two-step martensitic transformations again. This behavior has not been recognized in NiTi single crystals in literatures. It can be related to the heterogeneity of composition and stress fields around Ni_4Ti_3 precipitates.

Introduction

NiTi-shape memory alloys have superior-shape memory effect and super elastic behavior because of the thermo-elastic and the reversible martensitic transformation [1–3]. The high-temperature phase austenite with the B2 structure, on cooling, transforms to low-temperature phase martensite with the B19' structure. During heating reverse transformation of martensite to austenite occurs. Aging of the Ni supersaturated NiTi alloy produces Ni_4Ti_3 precipitates in the microstructure, in the presence of which the material shows two consecutive martensitic phase transitions, from the austenite high-temperature phase via the intermediate trigonal the R-phase to the monoclinic B19' martensite [1–4]. The formation of the R-phase can occur in the presence of (i) stress fields surrounding coherent

Ni_4Ti_3 precipitates, (ii) microstructural and chemical heterogeneity, (iii) stress fields around dislocations induced by cold working. Only in ternary alloys such as NiTiFe, NiTiAl, or NiTiCo the R-phase is known to occur spontaneously [1–7].

Nishida et al. [2] related the multiple-step martensitic transformation to the heat treatment atmosphere. Presented theories about the multiple-step martensitic transformation can be categorized in three groups:

- (1) Both the R-phase and the B19'-phase nucleate around the Ni_4Ti_3 precipitates and then grow into the parent phase. The R-phase grows smoothly and continuously, but the B19'-phase nucleates in a sudden burst and grows rapidly to its significant size, therefore it requires a high undercooling. Bataillard et al. [6] presented the theory based on coherent stress fields around the Ni_4Ti_3 particles. Presence of the stress fields were confirmed using the transmission electron microscopy (TEM) [8, 9]. The measured characteristic temperatures of the martensitic transformation near Ni_4Ti_3 particles were higher than in the regions far from the particles. Gall et al. [7] reported that coherent stress fields around the Ni_4Ti_3 particles assist the formation of specific variants of martensite phase. Bataillard et al. supposed that the first peak on cooling relates to the B2 \rightarrow R transformation; the R-phase nucleates at particle/matrix interfaces and grows toward the matrix. The second peak implies to the transformation of R \rightarrow B19'. This transformation occurs only in regions near Ni_4Ti_3 precipitates which are affected by coherent stress fields. The third peak relates to the R \rightarrow B19' transformation and occurs in the regions that are free of coherent stress fields [10–14].

J. Khalil-Allafi (✉) · B. Amin-Ahmadi
Research Center for Advance Materials, Faculty of Materials Engineering, Sahand University of Technology, Tabriz, Iran
e-mail: allafi@sut.ac.ir; jallafi@yahoo.de

- (2) Khalil-Allafi et al. [15] related the multiple-step martensitic transformation to the combination of two main parameters: (i) Ni-depletion of the matrix due to the formation and growth of Ni_4Ti_3 particles. This phenomenon was confirmed by Yang et al. using a combination of analytical TEM techniques [11]. (ii) The difference in nucleation barriers between the R-phase (about 1% shear strain) and the $\text{B}19'$ -phase (about 10%). Khalil-Allafi et al. [16] also proposed an explanation using the TEM results which show heterogeneous nucleation of Ni_4Ti_3 particles on grain boundaries. They reported that the first peak in DSC curves on cooling relates to the formation of the R-phase in the regions with Ni_4Ti_3 precipitates. The second peak is due to the formation of the $\text{B}19'$ -phase in the regions containing precipitates and the third peak relates to the transformation of the B2 to the $\text{B}19'$ -phase in the grain interior which are free from the Ni_4Ti_3 precipitates [12–17].
- (3) Fan et al. [12] suggested a theory based on the explanations of Bataillard et al. and Khalil-Allafi et al. This theory was proposed by small-scale heterogeneities due to the formation of closely spaced Ni_4Ti_3 precipitates in the matrix. They performed two series of aging experiments at 773 K using NiTi single crystals with the 50.6 and 51.5 at.% Ni. The aging time was chosen in the range of 1–150 h, they only found two-step martensitic transformations in their experiments. They produced polycrystals by cold working followed by the recrystallization process on NiTi single crystals. They observed three-step martensitic transformations in polycrystals and concluded that the precipitation along grain boundaries plays an important role in multiple-step martensitic transformations. The sequence of martensitic transformations in NiTi polycrystals according to their theory is the same sequence which was reported by Khalil-Allafi et al. and Dlouhy et al. previously [16, 17].

Michutta and Dlouhy et al. [18] using in situ cooling TEM reported that the R-phase nucleates at all precipitate/matrix interfaces and then the R-phase grows continuously toward the matrix. But, the $\text{B}19'$ martensite does not nucleate at all precipitate/matrix interfaces. They observed a sudden growth of the $\text{B}19'$ -phase from a precipitate/matrix interface in these alloys. This difference between the nucleation and the growth of the R-phase and the $\text{B}19'$ -phase is due to the small nucleation barrier of the R-phase; on the other hand, in an aged specimen under a stress, containing the small inter-particle spacing, the formation of the $\text{B}19'$ -phase is much more difficult and requires a significant undercooling. The $\text{B}19'$ -phase propagates in small

sudden jumps (step size of the order of 1 μm) through the free spaces between the precipitates [19, 20].

In polycrystals, the nucleation barrier at grain boundaries or on small defects, in comparison with the interior of grain, is small. In low super saturations, the nucleation rate in grain boundaries is considerable higher than the interior of grains; however, in high super saturation, there is no noticeable difference between the nucleation rate in grain boundaries and the interior of grains [12, 13]. Therefore, if the Ni content becomes low (50.6%), the nucleation rate at the grain boundary will be higher than the interior of the grain; thus, Ni_4Ti_3 particles precipitate along the grain boundaries and interior of the grains will be free of precipitates. When the Ni content increases to 51.5 at.%, differences between the nucleation rate in grain boundaries and the interior of grains decrease; therefore, the nucleation and the formation of Ni_4Ti_3 precipitates occur simultaneously. It leads to a homogenous distribution of Ni_4Ti_3 precipitates. Therefore, the martensitic transformation during cooling occurs in two steps [12, 13]. In NiTi polycrystals with low Ni content, Ni_4Ti_3 particles precipitate on grain boundaries and the interior of grains will be free of precipitates; therefore, two-step martensitic transformation $\text{B}2\text{-R-B}19'$ occurs at grain boundaries and a single-step martensitic transformation $\text{B}2 \rightarrow \text{B}19'$ occurs in the regions free of precipitates.

In this study, the multiple-step martensitic transformation in the NiTi single crystal alloy with Ni content of 51 at.% using the DSC method was investigated.

Materials and methods

A NiTi single crystal with the nominal composition of 51 at.% Ni was used. The specimen after solution annealing treatment at 850 °C for 30 min and water quenching was subjected to the aging treatment at 400 °C for various times. Aging treatments were performed by a muffle furnace without protective atmosphere. The samples were quenched into the water tank after each aging treatment. In order to determine the characteristic temperatures, DSC experiments were performed using type 2920 CE DSC from TA instruments.

The detail of experimental procedure was as following: the specimen was aged at 400 °C for 10 min and the DSC experiment was performed. Then the same specimen was aged again at 400 °C for various times, up to 50 h. The DSC experiment after each aging treatment was done. The DSC specimen (77 mg) was heated up to 120 °C, where it was held for 3 min. Then the DSC measurement was started by cooling the specimen down to -120 °C with a cooling rate of 10 °C min^{-1} . At -120 °C the specimen

was held for 3 min and then was heated up to 120 °C with a heating rate of 10 °C min⁻¹.

TEM was performed using a Philips CM20 analytical microscope operating at 200 kV in combination with a heating/cooling holder which allowed to adjust precise specimen temperatures and to observe the growth of transformed regions. TEM specimens were carefully mechanically ground to a thickness of 120 μm before disks of 3-mm diameter were stamped out and then electro polished using a double jet thinning technique (Tenupol; Struers A8 electrolyte at 20 V and intermediate flow rate).

Results and discussion

Figure 1 shows the DSC curve of the single crystal specimen subjected to the solution treatment at 850 °C for 30 min and water quenching. After the solution treatment during cooling and heating cycles, single-step B2 → B19' and B19' → B2 transformations occurred, respectively. The characteristic temperatures were:

$$M_s = -57\text{ }^\circ\text{C}, \quad M_f = -90\text{ }^\circ\text{C}, \quad A_s = -55\text{ }^\circ\text{C} \quad \text{and} \\ A_f = -18\text{ }^\circ\text{C}$$

Figure 2 presents DSC results of the aged single crystal specimen at 400 °C for 10, 20, 30, and 45 min. DSC results in Fig. 2 show two-step martensitic transformations during cooling and heating cycles. It is well known that in aging of nickel-rich NiTi alloys, due to formation of fine and coherent Ni₄Ti₃ precipitates within the B2 microstructure, the formation of the R-phase will be favored during the cooling. It is shown that the tendency of the R-phase formation increases in the presence of precipitates [14–16]. Therefore, during cooling in the first step B2 transforms to R-phase and with further cooling the R-phase transforms to B19'. In the heating cycle, the reverse transformation occurs from B19' to B2 via intermediate R-phase.

It was observed that with increase of the aging time up to 45 min at 400 °C all transformation temperatures increase. It can be explained by considering that with

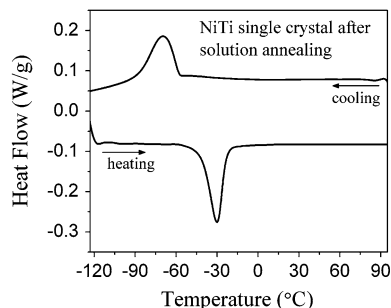


Fig. 1 DSC chart of Ni₅₁Ti₄₉ single crystal after solution annealing at 850 °C for 30 min and water quenching

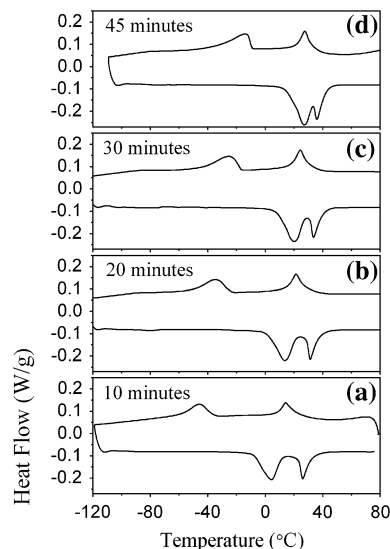


Fig. 2 DSC charts of Ni₅₁Ti₄₉ single crystal after aging at 400 °C for 10, 20, 30, and 45 min

formation of nickel-rich precipitates, nickel concentration within the matrix decreases and low nickel concentration leads to the high transformation temperatures [4, 17].

In DSC curves of the specimen aged at 400 °C for 1.25–4 h (Fig. 3), in the cooling cycle, the martensitic transformation occurs in three steps. This can be explained in the NiTi polycrystals according to the microstructural heterogeneity in microscopic or macroscopic level. The main reasons for multiple-step martensitic transformations can be categorized as following: (i) The gradient of nickel concentration in the vicinity of Ni₄Ti₃ precipitates [15–17], (ii) stress fields around Ni₄Ti₃ precipitates [6], and (iii) internal stress fields associated with heterogeneous

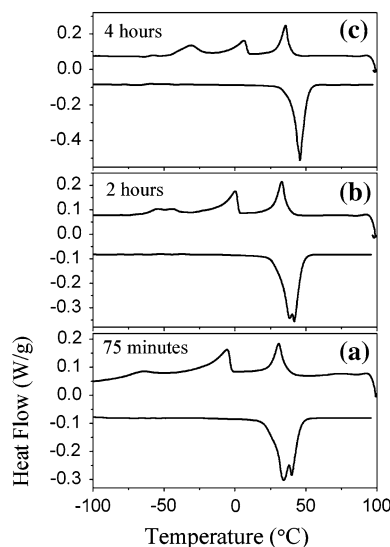


Fig. 3 DSC charts of Ni₅₁Ti₄₉ single crystal after aging at 400 °C for 1.25, 2, and 4 h

dislocation arrangements [20]. However, from macroscopic point of view, the heterogeneous precipitation of particles close to the grain boundaries might cause three-step transformations [15–17]. In the heating cycle, the reverse transformation for the aging time of 1.25 and 2 h, occurs in two steps. With increasing the aging time to 4 h, the reverse transformation occurs in a single step and it seems the B19' martensite phase directly transforms to B2 austenite phase without formation of the R-phase.

For investigation of the three-step martensitic transformation which observed in the DSC measurement for the sample, aged at 400 °C for 2 h, in situ TEM cooling experiments were performed. Figure 4 shows the TEM bright-field images and electron diffraction patterns, which taken at different temperatures. According to the DSC measurement (Fig. 3b), at 55 °C, no transformation occurs and the sample is still in the austenitic state. The TEM micrograph confirms that at 55 °C, B2 is the stable matrix phase and Ni₄Ti₃ particles are present in the matrix (Fig. 4a, a'). At 42 °C, at the beginning of the first DSC peak on cooling, the matrix has started to transform into the R-phase at the Ni₄Ti₃ particles/matrix interface, as indicated by the appearance of weak extra spots at 1/3 <1 1 0> in the electron diffraction pattern (Fig. 4b').

In the end of the second DSC peak on cooling (at –15 °C), further growth of the R-phase near the Ni₄Ti₃ precipitates can be observed. Besides, the spots at 1/3 <1 1 0> in the electron diffraction pattern have been strengthened (Fig. 4c'). With further cooling (at –45 °C) the R-phase starts to transform into the B19' phase (third peak).

Therefore, by the third DSC peak on cooling, most of the R-phase has transformed into B19' phase. In the corresponding diffraction pattern of this TEM micrograph, 1/2 <1 1 0>-type martensite reflections appear and the 1/3 <1 1 0>-type reflections of the R-phase disappeared (Fig. 4d').

Figure 5 shows DSC curves for the NiTi single crystal specimen after aging at 400 °C for 8 and 50 h. The DSC results indicate that with increasing aging time (8 and 50 h), the martensitic transformation in the cooling cycle occurs again in two steps and in the heating cycle occurs in

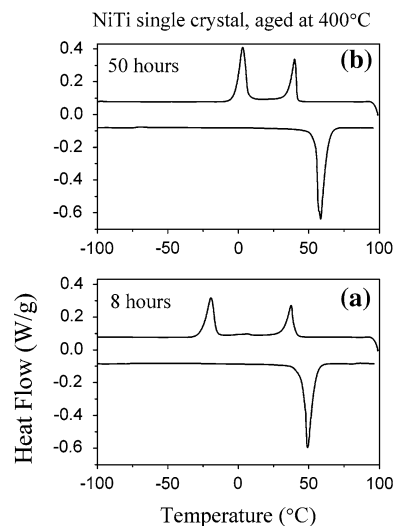


Fig. 5 DSC charts of Ni₅₁Ti₄₉ single crystal after aging at 400 °C for 8 and 50 h

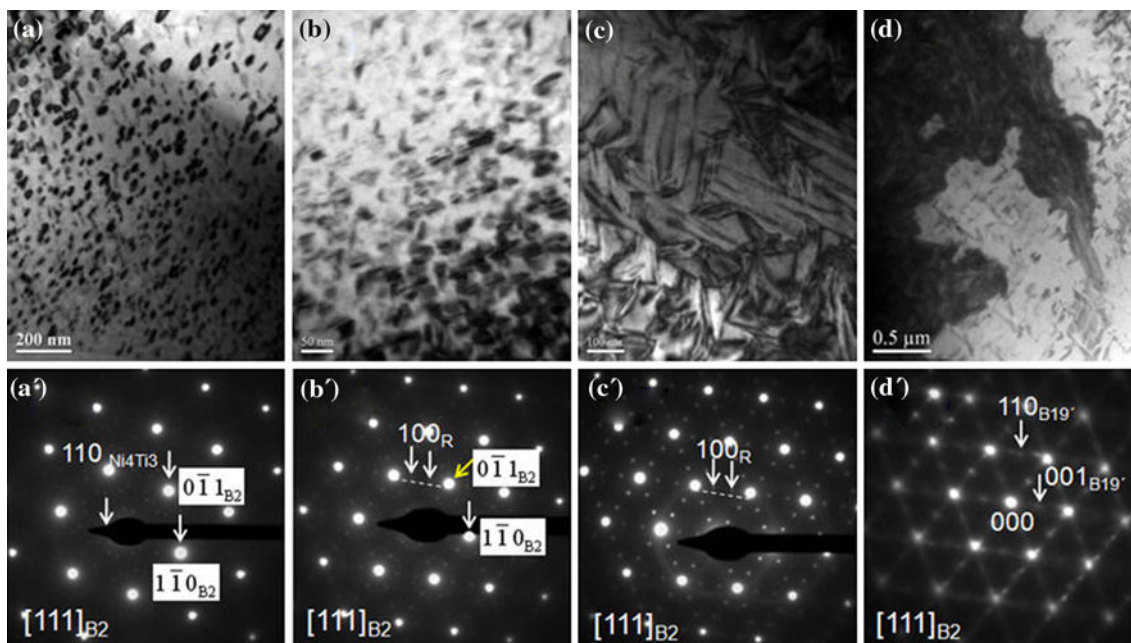


Fig. 4 a–d Bright-field TEM images and a'–d' corresponding diffraction patterns, taken in the [1 1 1] zone-direction of the B2- phase during cooling at a, a' 55 °C; b, b' 42 °C; c, c' –15 °C; and d, d' –45 °C

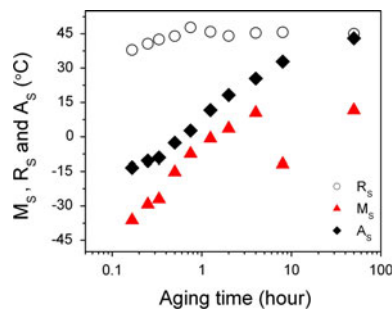


Fig. 6 Variations of characteristic temperatures versus aging time for $\text{Ni}_{51}\text{Ti}_{49}$ single crystal

one step. However, in the NiTi single crystal multiple-step martensitic transformations show 2-3-2 behavior with aging time at a constant aging temperature which reported in literatures for polycrystals [4, 15–17].

The variation of characteristic temperatures (M_S , R_S , and A_S) as a function of aging time at 400 °C for the NiTi single crystal have been shown in Fig. 6. It can be seen the M_S and A_S temperatures shift continuously to high temperatures with increasing aging time, but the temperature of the peak of the R-phase (R_S) reaches a constant value after 45 min of the aging time. It seems that the R-phase nucleates at the interface between B2 matrix and Ni_4Ti_3 precipitates, where the Ni content of the B2 matrix adjacent to the precipitate is constant with aging time.

The variation of transformation temperatures and sequence of martensitic transformations can be explained by formation of fine, coherent, and metastable Ni_4Ti_3 precipitates during aging treatment of Ni-rich NiTi alloys. Formation of Ni_4Ti_3 precipitates has two basic effects on the microstructure:

- (i) The change of Ni concentration around metastable Ni_4Ti_3 precipitates. Ni-depletion of the matrix with increasing aging time leads to increase of transformation temperatures.
- (ii) Existence of coherency stress fields around Ni_4Ti_3 precipitates. Stress fields around precipitates have more effect on the B19' martensitic transformation because of higher transformation strains of B19' formation (10%). It is clear that with increasing aging time Ni_4Ti_3 precipitates grow, the space between precipitates increases, they lose their coherency and this affect the transformation temperatures and the sequence of martensitic transformations.

As can be seen from Fig. 6, M_S temperature decreases in the specimen subjected to aging time of 8 h. This is due to change of sequence of transformations from three to two steps. This means that the second and third peak of martensitic transformations during cooling changes to a single peak.

Our results show that unlike findings of Fan et al., three-step martensitic transformations can occur in Ni-rich NiTi single crystals at intermediate aging times. Fan et al. did not observe three-step martensitic transformations in NiTi single crystals. It seems that they had not chosen proper intermediate aging times in their experiments. The critical range of intermediate aging time to obtain multiple-step martensitic transformations depends on two parameters; (i) the aging temperature and (ii) the Ni content of NiTi alloys [13–15]. With increasing the Ni content of NiTi alloy, the essential aging time to enhance multiple-step martensitic transformation decreases.

Michutta et al. observed the multiple-step martensitic transformations in the single crystal of NiTi specimen subjected to stress-assisted aging. According to the TEM observation of Michutta et al. and Dlouhy et al., when the distance of particles exceeds from a critical value (200 nm), the martensitic transformation during cooling occurs in three steps [19, 20].

Therefore, it can be concluded that multiple-step martensitic transformations can occur in aged Ni-rich NiTi single crystals with a homogeneous distribution of the Ni_4Ti_3 particles in the absence of large-scale microstructural heterogeneities. Findings of Fan et al. that small-scale microstructural heterogeneities cannot lead to multiple-step martensitic transformations are in contrary to results of Dlouhy et al. [12] and results of this study. The heterogeneous precipitation of Ni_4Ti_3 particles along grain boundaries represents large-scale microstructural heterogeneities and is responsible for the multiple-step martensitic transformation in NiTi polycrystals. In the NiTi single crystals, other types of microstructural heterogeneities have been identified such as differences in the chemical composition between dendrite and inter-dendrite regions. Therefore, there is a general agreement on the fact that heterogeneities in the microstructure of NiTi alloys cause multiple-step martensitic transformations [5, 12, 13, 16–21]. In NiTi single crystals, increasing aging time results in the growth of Ni_4Ti_3 precipitates and the space between precipitates increases. Up to critical value of Ni_4Ti_3 precipitates size, martensitic transformations during cooling occurs in two steps. When the size of Ni_4Ti_3 precipitates reaches the critical value, three-step martensitic transformations occur. Further growth of precipitates for high aging time results in two-step martensitic transformations again. This is may be due to the formation of incoherent Ni_4Ti_3 precipitates for high aging times.

Conclusions

We investigated the influence of aging time at 400 °C on the features of martensitic transformations of the $\text{Ni}_{51}\text{Ti}_{49}$

single crystal as measured using DSC. There is an evolution of DSC curve features with the aging time. For short aging times between 10 and 45 min at 400 °C, two DSC peaks were obtained during cooling from the austenite phase. For intermediate aging times (1.25–4 h), three-step martensitic transformation occurs and for high aging times (8 and 50 h) during cooling martensitic transformations occurs in two steps again. This means that multiple-step martensitic transformations in the single crystal NiTi alloys show 2-3-2 behavior with aging time. This behavior is similar to martensitic transformations in polycrystals during cooling as reported previously [4, 14–16]. The explanation for variation of transformation temperatures and sequence of martensitic transformations is given by formation of fine, homogenous, coherent, and metastable Ni₄Ti₃ precipitates during aging treatment of Ni-rich NiTi alloys.

Increasing aging time leads to increase of M_S and A_S temperatures due to Ni-depletion of matrix. However, R_S reaches a constant value after 45 min of aging time. It can be related to the nucleation of the R-phase at the interface between B2 matrix and Ni₄Ti₃ precipitates, where the Ni content of the B2 matrix adjacent to the precipitate is constant for different aging times.

Acknowledgements Jafar Khalil-Allafi thanks Professor Gunther Eggeler, Dr. Christoph Somsen and Dr. Andreas Kroeger from Ruhr University Bochum, Germany for assistance (supply of the NiTi single crystal, TEM investigations).

References

1. Kim JI, Liu Y, Miyazaki S (2004) *Acta Mater* 52:487
2. Nishida M, Hara T, Ohba T, Yamaguchi K, Tanaka K (2003) *Mater Trans A* 12:2631
3. Kurumada M, Kimura Y, Suzuki H, Kido O, Saito Y, Kaito C (2004) *Scripta Mater* 50:1413
4. Eggeler G, Khalil Allafi J, Gollerthan S, Somsen Ch, Schmahl W, Sheptyakov D (2005) *Smart Mater Struct* 14:S186
5. Zheng Y, Jiang F, Hong Yang L, Liu Y (2008) *Acta Mater* 56:736
6. Bataillard L, Bidaux J-B, Gotthardt R (1998) *Philos Mag* 78:327
7. Gall K, Sehitoglu H, Anderson R, Karaman I, Chumlyakov YI, Kireeva IV (2001) *Mater Sci Eng A* 317:85
8. Tirry W, Schryvers D (2009) *Nat Mater* 8:752
9. Tirry W, Schryvers D (2005) *Acta Mater* 53:1041
10. Zhou Y, Fan G, Zhang J, Ding X, Ren X, Suna J, Otsuka K (2006) *Mater Sci Eng A* 438:602
11. Yang Z, Tirry W, Schryvers D (2005) *Scripta Mater* 52:1129
12. Fan G, Chen W, Yang S, Zhu J, Ren X, Otsuka K (2004) *Acta Mater* 52:4351
13. Otsuka K, Ren X (2005) *Prog Mater Sci* 50:511
14. Tadaki T, Nakat Y, Shimizu K, Otsuka K (1986) *Trans JIM* 27:731
15. Khalil-Allafi J, Ren X, Eggeler G (2002) *Acta Mater* 50:793
16. Khalil-Allafi J, Dlouhy A, Eggeler G (2002) *Acta Mater* 50:4255
17. Dlouhy A, Khalil-Allafi J, Eggeler G (2003) *Philos Mag* 83:339
18. Michutta J, Ch Somsen, Yawny A, Dlouhy A, Eggeler G (2006) *Acta Mater* 54:3525
19. Dlouhy A, Bojda O, Somsen Ch, Eggeler G (2008) *Mater Sci Eng A* 481:409
20. Kroger A, Dzaszyk S, Frenzel J, Somsen Ch, Dlouhy A, Eggeler G (2008) *Mater Sci Eng A* 481:452
21. Morawiec H, Stroz D, Goryczka T, Chrobak D (1996) *Scripta Mater* 35:485